JASs *R*eports
Journal of Anthropological Sciences
Vol. 88 (2010), pp. 129-150

The association between dental mineralization and mandibular form: a study combining additive conjoint measurement and geometric morphometrics

Michael Coquerelle[1,2], Priscilla Bayle[3,4], Fred L. Bookstein[1,5], José Braga[2], Demetrios J. Halazonetis[6], Stanislav Katina[1,7] & Gerhard W. Weber[1]

1) Department of Anthropology, University of Vienna, 1090 Vienna, Austria
e-mail: michael.coquerelle@univie.ac.at

2) Anthropologie Moléculaire et Imagerie de Synthèse, FRE 2960, Université Paul Sabatier, 31000 Toulouse, France

3) Research Department of Cell and Developmental Biology, UCL, London WC1E 6BT, UK

4) Département de Préhistoire, UMR 7194-USM 204, Muséum National d'Histoire Naturelle, 75013 Paris, France

5) Department of Statistics, University of Washington, Seattle, Washington 98195, U.S.A.

6) Orthodontic Department, University of Athens Dental School, 11527 Athens, Greece

7) Department of Applied Mathematics and Statistics, Faculty of Mathematics, Physics and Informatics, Comenius University, Mlynska dolina, 842 48 Bratislava, Slovakia

Summary - *Studies have suggested that dental development substantially influences the variation of mandibular morphology and growth in primates. As a contribution to the methodology of such studies, we introduce a novel approach to quantifying the covariation between teeth and mandible. This was done showing fluctuations in the magnitude of this covariation within a sample of modern human mandibles at different postnatal ages. Dense CT-derived mandibular surface meshes of 73 females and 71 males, ranging in age from birth to adulthood, were processed by methods of geometric morphometrics. Each specimen's deciduous and permanent teeth were rated for mineralization stage. Form-space principal component analysis of the morphometric data was used to produce a single metric variable that best explains mandibular-form variation. This variable was then used to quantify the developing teeth, all together, through the use of the additive conjoint measurement method. This new metric variable corresponds to the dental prediction of the mandibular-form variation. Finally, we examine the covariation of the two over the full range of mineralization stages. We found a strikingly tight association between mandibular form and dental maturation up through the full emergence of the deciduous dentition (about age 2 y.), followed by an equally striking decline in that association in later developmental stages, particularly for girls. The onset of the decline of the teeth-mandible relationship coincides with the onset time of the adult-like pattern of mastication and speech. The increasingly functional diversity may lead to more independence between dental development and mandibular growth than during the first two years.*

Keywords - *Dentition, Mandible, Modern humans, Growth, Covariation*

Introduction

Among extant primates, the great apes have a prognathic face with large jaws and teeth adapted for powerful mastication, whereas in humans, the face is orthognathic, the dental arcade reduced and the correspondingly smaller jaw is committed to two functions, mastication and speech.

The onset, duration and rate of tooth mineralization and tooth eruption sequence are quite distinct between these two groups (Robinow *et al.,* 1942; Nissen & Riesen, 1945, 1964; Dean & Wood, 1981; Aiello & Dean, 1990). While it is assumed that dental development significantly influences the variation of mandibular morphology and growth in primates (Dean & Beynon 1991, Taylor 2002; Taylor & Groves 2003), details of this relationship over time are still scarce. Therefore, the study of the pattern of covariation between developing teeth and the growing mandible may provide useful insights into mandibular shape variations among primates.

The strong association between dental development and mandibular growth is not surprising for many reasons. From an embryological point of view, teeth and mandible are derived tissues that both stem from the first pharyngeal arch (Lumsden, 1988; Atchley & Hall, 1991; Schwartz & Dean, 2000; Dean, 2006). One would then expect suitable pairs of measures of both tissues to be correlated over development because of their common origin. More mechanistically, the interrelated development of mandible and teeth throughout prenatal and postnatal life is an example of the functional matrix hypothesis (Moss & Young, 1960; Moss, 1962; Enlow, 1990): as long as teeth continue to develop, there is a need for more jaw space.

A characteristic of this integrated developmental system would be that the coordination between teeth and mandible should be tighter during earlier developmental stages than at later ages (Boughner & Hallgrímsson, 2008). This expectation is based on the gradual loss of synchronicity over time between the "cerebral clock", controlling the circadian rhythm of the body, and the distinct "peripheral clocks", such as the "dental clock" and the "mandibular clock", controlling the rhythm of the dental and mandibular cells respectively. If the association between these developmental clocks relaxes during ontogeny, as was assumed by Boughner & Hallgrimsson (2008), one might expect that, at the macrostructural level, the covariation between dental mineralization and mandibular form should be seen to relax as well.

Functions play an active role in mandibular growth. In humans, chewing requires high occlusal forces during the lateral movement of the jaw. These forces are produced by the synchronous coactivation of agonistic muscles (*e.g.*, the masseter and the temporalis) and reciprocal activation among antagonistic muscles (*e.g.*, the masseter and the digastrics) (Moore *et al.*, 1988). Speech, in contrast, requires lesser occlusal forces than chewing, approximately 20% of the maximum chewing forces (Wilson *et al.*, 2008), because the muscle synergies are different: there is no reciprocal activation among antagonistic muscles, but rather an antagonistic coactivation (Moore *et al.*, 1988). In addition to the difference in force magnitudes, the variability in patterns of muscle activation is greater during speech than during mastication (Moore *et al.*, 1988). One might therefore expect that, during growth, the association between teeth and mandible might also fluctuate over the course of development of these functions.

Little attention has been given to document the relationship between the teeth and jaw at macrostructural level during postnatal development. To the best of our knowledge, there are no quantitative summaries available of the interdependency between dental development and mandibular growth, nor has there been any division into periods of high versus low covariation. Several studies have reported correlations between dental development and other maturational criteria in humans, for example, between mandibular tooth mineralization and hand-wrist maturation (Uysal *et al.*, 2004) or cervical vertebra maturation (Başaran *et al.*, 2007). In both of these studies, each tooth was evaluated separately and correlation coefficients with the bone measures ranged from 0.6 to 0.8. However, during development or function, the mandible interacts not with independent teeth but with the dentition as a whole. One possible approach taking this into account would be to aggregate degrees of mineralization over the dental sequence (Braga & Heuzé, 2007), an approach that further permits considerations about onset, duration and rates of mineralization among the teeth. To evaluate the strength of the relationship between teeth and mandible during

development, one can scale the teeth, all together, against mandibular form variation and measure the amplitude or the power of the scaling.

To this end, our exploratory study presents a novel approach to quantifying the covariation between jaw and teeth in modern humans by borrowing a statistic from psychometrics which we then combine with morphometrics. From a sample of CT-scanned living humans, ranging from birth to adulthood, each specimen's dental sequence was determined by a set of qualitative variables, one per tooth, coding for the level of crown and root mineralization. In this analysis, (i), CT-derived mandibular surface meshes are processed by geometric morphometric methods in order to produce, via form-space analysis (Mitteroecker *et al.*, 2004), a single metric variable that best explains mandibular form variation during postnatal development; (ii), for each tooth and each mineralization stage, a weight is calculated as the average of the composite variable computed in (i); and (iii), for each specimen's dental sequence, these tooth weights are averaged over the dental sequence. In this way, each specimen's dental sequence is characterized by a number in units of mandibular form, and the numbering over all the specimens, taken together, represents a metric proxy of dental development in units of jaw form: a *dental* predictor of mandibular form, which we examine over the range of mineralization stages. Steps (ii) and (iii) are an adaptation of a psychometric method, the additive conjoint measurement method (Luce & Tukey, 1964). This technique is explained in detail in the following section.

Materials and methods

Mandibular surfaces

Our study included computed tomography (CT) of 144 modern humans (73 females and 71 males) of mixed ethnicity, living in France, ranging in age from birth to adulthood (Tab. 1). The CT scans were provided by the Pellegrin Hospital (Bordeaux), the Necker Hospital (Paris), and the Clinique Pasteur (Toulouse). The CT scans were acquired via a variety of devices: Mx Twin® from Picker and Mx800 IDT16® from Philips (Clinique Pasteur), Brillance CT40® from Philips (Pellegrin Hospital), and Lightspeed VCT® from GE Healthcare (Necker Hospital). All CT scans were recorded in DICOM file format at a reconstruction matrix size of 512 by 512 pixels. Pixel size ranged from 0.23 to 0.66 mm and slice thickness from 0.30 to 0.70 mm. These individuals had been referred for cranial trauma, inflammation of maxillary sinuses or neonatal distress but were found to be free of reportable abnormalities. The CT scans were anonymized by the medical institutes, except for information regarding age and gender. The use of these data for our present purpose was approved by French institutional boards.

The half-maximum height protocol (Spoor *et al.*, 1993) was used to reconstruct each mandibular surface from the CT scans via the software package Amira (Mercury Computer Systems, Chelmsford, MA). This protocol samples the Hounsfield values on either side of the transition between two adjacent tissues and takes the mid value between the two as a threshold. The youngest specimens had areas with different mineralization levels, requiring local adjustments of this threshold value. The reconstructed mandibular halves of the youngest specimens that showed incomplete ossification of the symphysis were fused virtually by cubic interpolation of the surface from each side of the symphyseal cartilage. All reconstructions were done by the same investigator (MC).

Rating dental development

The degree of mineralization of each tooth was assessed by two of us (MC and PB) using the rating system elaborated by Demirjian *et al.* (1973) for the permanent dentition and as modified by Liversidge & Molleson (2004) for the deciduous dentition as well. Both rating systems subdivide tooth development into stages based upon mineralization of crown and root. Each stage is assigned a letter, lower case for deciduous teeth and upper case for the permanent teeth. The lettering starts with *a* or *A*, the beginning of crown

Tab. 1 - Sample composition distributed according to dental stages (DS) and sex. For each group, the age range corresponds to the minimum and maximum values.

DS	Females	Age	Males	Age	Total
DS 1	9	0.0 - 1.0	8	0.1 - 1.1	17
DS 2	3	1.4 - 2.0	8	1.3 - 2.6	11
DS 3	12	2.3 - 6.0	13	2.4 - 5.8	25
DS 4	27	6.4 - 12.2	21	7.2 - 12.1	48
DS 5	12	10.7 - 14.6	11	11.0 - 14.5	23
DS 6	10	13.2 - 25.7	10	15.3 - 24.7	20

mineralization, and ends at *h* or *H*, the closure of the apex. Because the width of the deciduous root apex opening, originally assessed through radiographs (Liversidge & Molleson, 2004), could not be reliably estimated using CT scans, deciduous teeth at stage *h1* were rescored as stage *g*. Likewise, stage *h2* became stage *h*. Owing to the range of our sample, which contains specimens at birth and during the mixed dentition, three supplementary stages had to be defined: stage *0*, for the absence of calcification (tooth chamber visible or not) in deciduous and permanent dentition; stage *r*, for root exfoliation; and stage *x*, for loss of an exfoliated deciduous tooth. Consequently, there were 11 stages for deciduous tooth maturation and 9 stages for permanent tooth maturation. The stages are listed in Table 2.

The repeatability of these radiographic scoring systems for the CT, as for microCT data (see Bayle *et al.*, 2009a,b), was tested by five observers (MC, PB, JB, and two independent observers). A sample of five controlled cases (representing 40 teeth) from an archaeological collection, loaned by the Laboratoire d'Anthropologie des Populations du Passé from University Bordeaux 1 (France), was radiographed, CT-scanned and microCT-scanned. There were no meaningful differences between radiographic, CT and microCT data. Disagreement between observers was limited to one stage for CT images (Coquerelle *et al.*, 2007).

As there is no meaningful difference between right and left tooth macro-structural maturation (Moorrees *et al.*, 1963; Demirjian *et al.*, 1973; Heuzé 2004), we scored the left hemi-arch: from di1 to dm2 for the deciduous teeth, and from I1 to M3 for the permanent teeth.

We mentioned earlier that functions such as chewing play an active role in mandibular growth. In general, tooth emergence precedes the change in chewing behaviour and is likely to influence the development of rhythmic chewing (as suggested by experiments on other species: Iinuma *et al.*, 1991). Therefore, the examination of tooth emergence provides information regarding the functional advance of the jaws during growth. As is customary in anthropological studies (*e.g.*, Bastir & Rosas, 2004; Cobb & O'Higgins, 2007; Lieberman & McCarthy, 1999; McNamara & Graber; 1975; Kupczik *et al.*, 2009; Kurihara *et al.*, 1980; Shea, 1989), we subdivided the sample into six stages of maturation in terms of tooth emergence categories: DS1, before the complete emergence of the deciduous second incisor; DS2, before the complete emergence of the deciduous second molar; DS3, before the complete emergence of the permanent first molar; DS4, before the complete emergence of the permanent second molar (M2); and DS5, after the complete emergence of the permanent second molar but without complete mineralization through M2; and DS6, after the complete emergence of M2 and with a complete mineralization of all permanent teeth up through M2 (see Tab. 1).

Landmark and semilandmark data

Using the open-source software Edgewarp3D (Bookstein & Green, 2002), a 3D template of 415 points was created to capture the mandibular surface geometry. This template is an assemblage

***Tab. 2 - Tooth development stages based on Demirjian* et al. *(1973) and Liversidge & Molleson (2004), modified for this study. Stages* 0, r, *and* x *were added to the original scale and stage* h1 *was merged with* g.**

Stage	Description
0	Crypt formed but germ not visible.
a/A	Beginning of crown mineralization
b/B	Incisors and canine: Mineralized incisal edge/cusp tip has reached maximum mesiodistal width.
	Molars: Coalescence of cusp tips to form a regularly outlined occlusal surface.
c/C	Enamel formation is complete at the occlusal surface. Approximal edges of forming crown have reached future contact areas. The beginning of a dentinal deposit is seen.
d/D	Crown formation is completed down to the cemento-enamel junction, at least in lateral projection (i.e., at mesial and distal faces of the tooth)
e/E	Incisors, canine, molars: Root formation is more than a spicule, but root length is less than crown height.
	Molars: Initial formation of root bifurcation is seen in the form of a mineralized point or semilunar shape. Root length is less than crown height.
f/F	Incisors, canine, molars: Root walls are very thin, and root length is equal to or greater than crown height. Root length is incomplete, with diverging apical edges.
	Molars: Midway down root, root wall is thinner than root canal.
g/G	Incisors and canine: Root length is almost complete, but apical edges are parallel or slightly converging.
	Molars: Mesial root length is almost complete, but apical edges are parallel or slightly converging. Midway down root, root wall is thicker than root canal.
	Root length complete, with apical walls converging, but apex is still open (width = 1 mm).
h/H	Apical dentine edge is sharp; apex is only just visible/closed (width <1 mm).
r	Root resorption initiated.
x	Deciduous tooth exfoliated.

of 14 landmark points, 128 curve semilandmarks, and 273 surface semilandmarks that were digitized onto a typical specimen surface. Then, the same template was warped onto each specimen mandible by an iterative thin-plate spline. Figure 1 and Table 2 show this template on a typical right hemimandible.

As part of the digitization process, semilandmarks slide along curves and surfaces in such a way as to minimize the bending energy of the thin-plate spline interpolation function computed between each specimen and the sample Procrustes average (Bookstein, 1997; Gunz *et al.*, 2005). The iterative procedure approximates curves by sets of chords calculated as vectors of two neighbouring (semi)landmarks, and surfaces by their triangulations (Bookstein, 1997; Gunz *et al.*, 2005). Once estimated in this way, semilandmarks can be considered as homologous points for the purpose of the subsequent (Procrustes) steps.

Landmarks and semilandmarks were converted to shape coordinates by Generalized Procrustes Analysis (GPA: Rohlf & Slice, 1990; Bookstein, 1991). This involves translating, rescaling, and rotating the configurations relative to each other so as to minimize the overall sum of squared distances between corresponding (semi) landmarks. The rescaling adjusts the landmark coordinates so that each configuration has a unit centroid size (square root of the summed squared Euclidean distances from all (semi)landmarks to their centroid: Dryden & Mardia, 1998). The scale factor is preserved, in the form of its natural logarithm, for the principal component analysis in step 1 of the analyses listed below.

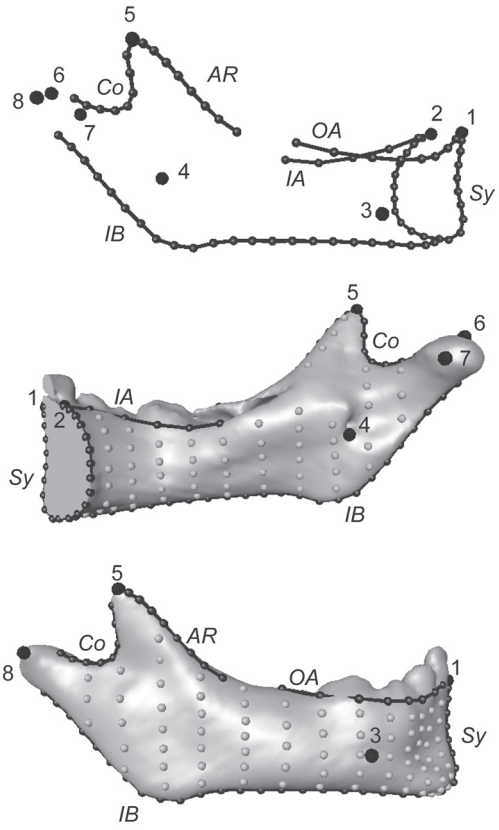

Fig. 1 - Mandibular template, right hemi-mandible. Top: landmarks (large black dots) and curve semilandmarks (small black dots and lines). Middle and bottom: right hemi-mandible of a specimen aged about 1 y with landmarks, curve semilandmarks and surface semilandmarks (grey dots). Names of the landmarks and curve semilandmarks are listed in Table 3.

Analyses

The statistical analysis consisted in 3 steps.

Step 1. A Principal Component Analysis (PCA) of the matrix of shape coordinates augmented by a column of the natural logarithm of centroid size (LnCS) – corresponding to a PCA in form space (Mitteroecker *et al.*, 2004) - was carried out on the whole sample. Form-space Principal Component 1 (FPC1) represents a "growth axis" whenever LnCS has a huge loading in this component, as was the case in our data. Our plots of the corresponding FPC scores are enhanced by a moving-average estimator of age-specific FPC averages using linear regressions on calendar age (see Bulygina *et al.*, 2006). The "average" FPC scores at 0.15, 0.5, 2, 4, 6, 8, 10, 12, 14, 16, and 18 years of age are actually regression estimates of this sort. But these regressions are not used in the course of later steps in the analysis. In fact, they only represent a visualization aid.

The next two steps of the analysis consist in scaling the teeth, all together, against FPC1. To this end, we adapt the Additive Conjoint Measurement method (ACM) of Luce & Tukey (1964). Originating in psychometrics, conjoint measurement theory supports the quantification of integrated properties of a system of multi-dimensional attributes when one of them can be highlighted as an "output". In the present study, the predictor domain is those dental sequences and the ouput is mandibular form as conveyed by FPC1. In the ACM method, each separate value of an attribute of a predictor (here, each tooth) is converted to a quantity in units of the output measure (here, along the scale of FPC1, namely, the average score on FPC1 for its particular mineralization stage). The overall coherence of the modelling is assessed by the success of summation of these scores over all the predictors – all the teeth, in this case – for predicting the actual FPC1 score. For more algebraic detail involving this class of methods, see Krantz *et al.* (1971).

The ACM method has a great deal in common with the nonlinear version of Partial Least Squares (PLS) that has been applied in other developmental contexts (*e.g.*, Bookstein *et al.*, 1996). It is not, however, the PLS based on the Singular-Value Decomposition (SVD) of a covariance matrix as commonly used in many studies (*e.g.*, Bastir & Rosas, 2006; Bastir, 2008; Bookstein *et al.*, 2003; Cobb & Baverstock, 2009; Gunz & Harvati, 2007; Mitteroecker & Bookstein, 2007; 2008; Rohlf & Corti, 2000). An SVD is least-squares, and so is this PLS, but in a quite different way. To help the reader navigate, we explain the method with the aid of a "toy example" (Fig. 2).

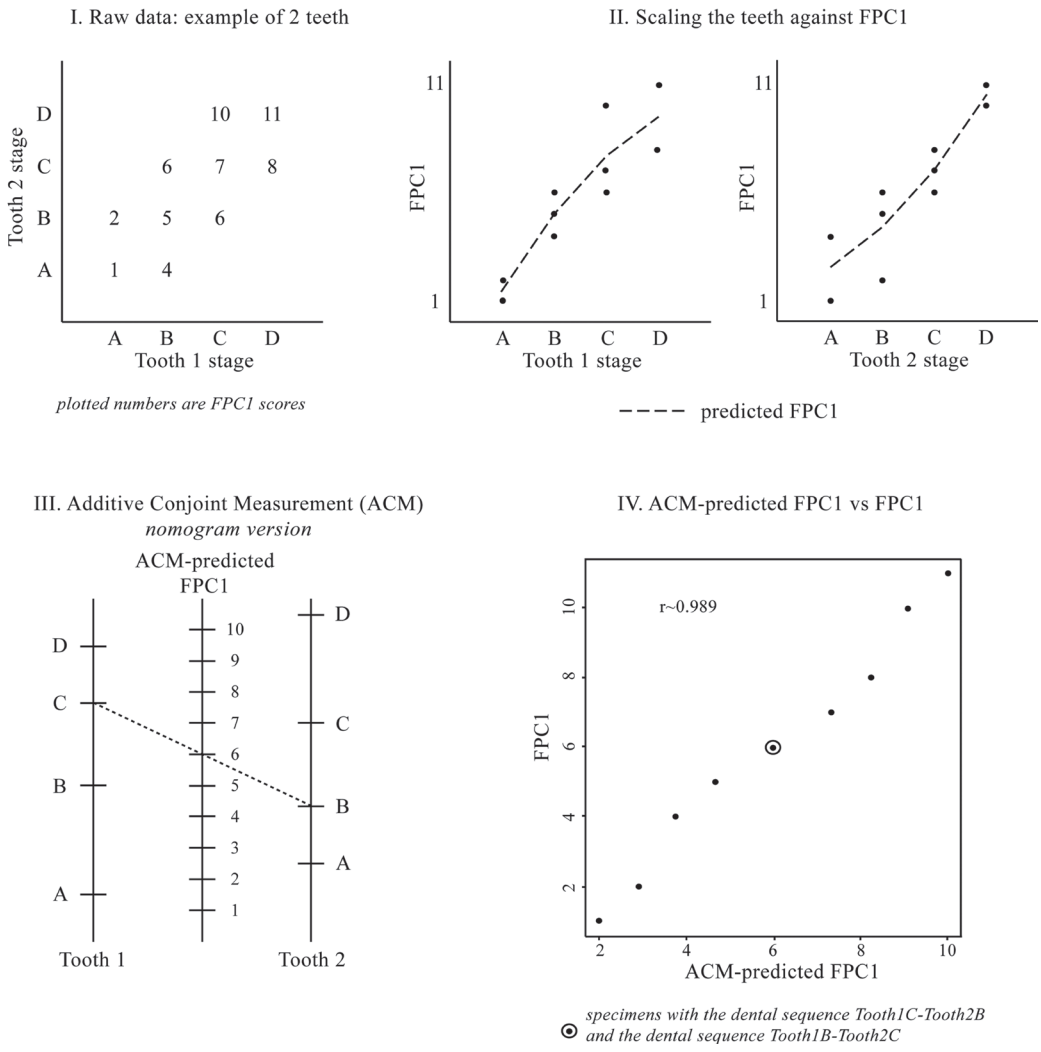

Fig. 2 - "Toy example" of the Additive Conjoint Measurement method. FPC1: Form-space Principal Component one.

The raw data for this example are as in Fig. 2.I. We have ten cases (in reality, there were 144) for which we assessed the mineralization stages for each of the two teeth (in reality, there were 5 deciduous and 8 permanent teeth). Each mineralization stage can take on one of four values A, B, C, D (in reality, there were up to 11 of these stages). As the figure shows, in our toy sample the stages are somewhat correlated across the teeth (which is also the case for our data), but the correlation is imperfect. The observed value of FPC1 rises with the stage of each tooth, but not linearly (also the case in our data). So the basic structure of the example is not so far from the reality of our dento-mandibular data set, except that the values of FPC1 happen to be all integers.

Step 2. For each tooth and each mineralization stage, we average the value of FPC1 for that subsample (Remember that FPC1 was computed completely without any reference to the tooth

mineralization data). Then we plot the resulting calibration in heavy dashed line for each tooth separately. As averages, these lines are each least-squares in the estimate of the average: that is one way to think about the phrase "least-squares" in "partial least squares" (PLS). As for the "partial", either of the two curves in Figure 2.II pertains to only *part* of the data. The heavy dashed lines in Figure 2.II represent a nonlinear rescaling of the original data as if each tooth, by itself, was predicting FPC1. For the real data, these averages are called FPC1 weights in Figures 4 and 5 and each tooth has a series of FPC1 weights that average the actual FPC1 observed over each of the mineralization stages (*0*|*a*|*A* to *h*|*x*|*H*) observed for that tooth. As in our example, Figure 2.II, these curves are monotonically increasing.

Step 3. The "additive" part of ACM arises in connection with the maneuver that is the subject of Figure 2.III. Here, taking advantage of the fact there are only two teeth in the toy example, we show the addition graphically, in the form of a *nomogram*. The dashed line connects the point for the scaled prediction from tooth 1 with the point for the scaled prediction for tooth 2 for a case with the dental sequence C, B. The middle of the line (average of the heights of its two endpoints) represents the numerical information about FPC1 in the two tooth stages separately. This average is the ACM prediction of FPC1 case by case. This prediction, too, takes the explicit form of a PLS computation, as it is the average of the predictions according to each predictor separately; that is another way of explaining how PLS averages univariate predictions. This ACM prediction of FPC1 is called the FPC1 composite weight in Figure 7.

We assess the adequacy of this "model" by the scatterplot in Figure 2.IV, which compares our ACM-reconstructed FPC1 to the actual FPC1 in Figure 2.I. For the real data (Fig. 7), we examined the analogous scatterplot to determine the apparent regression coefficient and corresponding regression error (error variance) between FPC1 composite weights and FPC1 scores - *i.e.*, between reconstructed and observed FPC1 scores - across two developmental periods defined according to M1 mineralization stages. We used M1-based developmental periods, instead of the classic maturation stages based on tooth emergence categories, so that identical mineralization sequences did not end up assigned to inconsistent stages. All the statistical analysis was programmed in R software. The R script of the ACM method is available upon request from the corresponding author.

Results

Step 1: Form-space PCA of mandibular growth

Figure 3 shows the first three components of the form-space PCA according to dental stages and sex. The first three axes account for approximately 95% of the total variance. FPC1 alone summarizes 92.6% of the variance as size-related shape change of the mandibular surface; its correlation with LnCS is r=0.994.

The sexes differ significantly in average form both at DS1 and at DS6, but not at any of the intermediate stages (permutation tests, 1000 permutations). These results are consistent with a form-space PCA analysis, which shows that male and female growth trajectories are shifted with respect to one another along the first axis, converging during DS1 but diverging by the beginning of DS4 (Fig. 3). Note, too, that the rate of female mandibular form change decreases after age 6 relative to that of the males, who appear to have a longer period of size-related shape change.

In the direction of FPC1 (Fig. 3), mandibular form variation in the subsample ranging from birth to the complete emergence of the deciduous dentition (transition between DS2 and DS3) is as large as that in the subsample ranging from DS3 to DS6, while the first period lasts just 2 years. The transition between the two periods corresponds to a clear change in the pattern of mandibular form variation.

Step 2: Coordination between mandibular form changes and each tooth

Figures 4 and 5 show the distribution of FPC1 weights for each tooth. Regarding deciduous

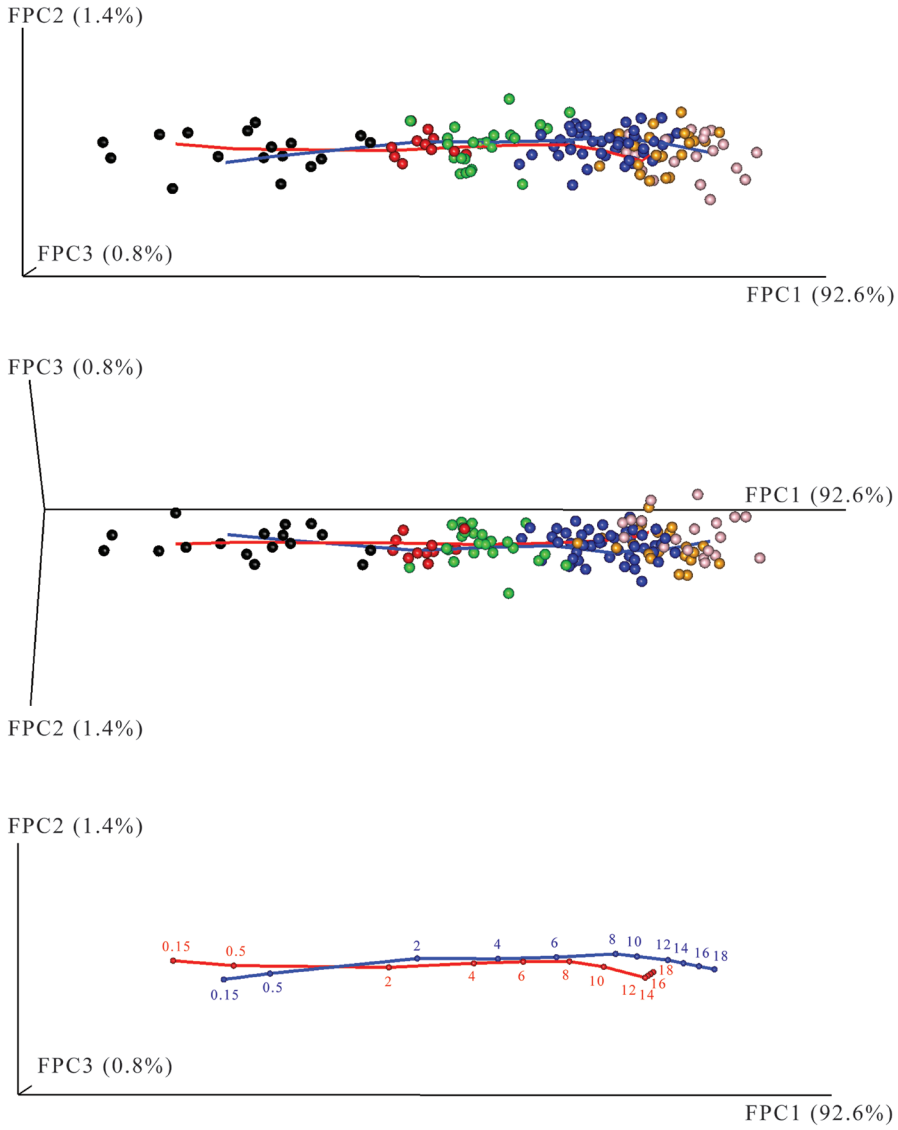

Fig. 3 - ***Form-space PCA. FPC1, FPC2 and FPC3 account for 94.8 % of the total variance. Black dots: DS1; red dots: DS2; green dots: DS3; blue dots: DS4; orange dots: DS5; pink dots: DS6. The red and blue lines represent respectively the female and male mandibular growth trajectories computed via linear regression of the PC scores on age (moving average algorithm). Bottom row: male and female growth trajectories with indicated ages.***

teeth (Fig. 4), FPC1 weights sorted perfectly against mineralization stages. The plots of actual FPC1 scores against FPC1 weights thus show a common trend, but note the large variance at the last two stages, *r* and *x* (because they represent the completion of development, or tooth loss, and thereafter staging remains constant even though mandibular form change continues).

For all permanent teeth, except M3, the average FPC1 weights sorted perfectly by stage whenever there was more than one specimen at that stage (Fig. 5). Regarding the teeth that begin their mineralization later – P3, P4 and M2 – stage *0* had a high variance (because we rated these teeth from birth, to avoid missing data) and is therefore less informative.

What we observed in the pooled sex sample was also observed within each sex separately (results not presented) except for the third molar (Fig. 6). In males, FPC1 means of M3 stages up to stage *E* were in correct order, but in females, stages *B* to *H* appear jumbled in relation to FPC1, probably because mandibular form change has ended.

Step 3: Additive Conjoint Measurement (ACM)

The results at step 2 permit us to produce a metric proxy for dental maturation, an FPC1 composite weight, by the ACM method (averaging of the FPC1 weights across teeth, individual by individual; recall that these FPC1 weights themselves are already FPC1 scores averaged across individuals sharing the maturation category tooth by tooth). The computation of the composite scale averages over observed stages *a*, *b*, *c*, *d*, *e*, *f*, *g* and *A*, *B*, *C*, *D*, *E*, *F*, *G*, and likewise stage *H* for teeth P3, P4 and M2 (for which stage *H* was found mainly in mandibles that nearly reached their final size). Appendix 1 presents all 91 different mineralization sequences from the pooled sex sample sorted according to FPC1 composite weights. Among our sample of 144 specimens, 54 sequences were seen more than once. For example, the specimens at DS6 had stage *H* for all the teeth (except for M3), and hence they had the same FPC1 composite weights.

We focused our correlation analysis on the age range from birth to 17 y – beyond this age there is very little mandibular form change. As the pattern of mandibular form variation changes after the complete emergence of the deciduous dentition (Fig. 3), we analyzed the covariation between tooth and jaw before and after that moment. In the earlier period, up to the transition from DS2 to DS3, are the M1 stages from *A*

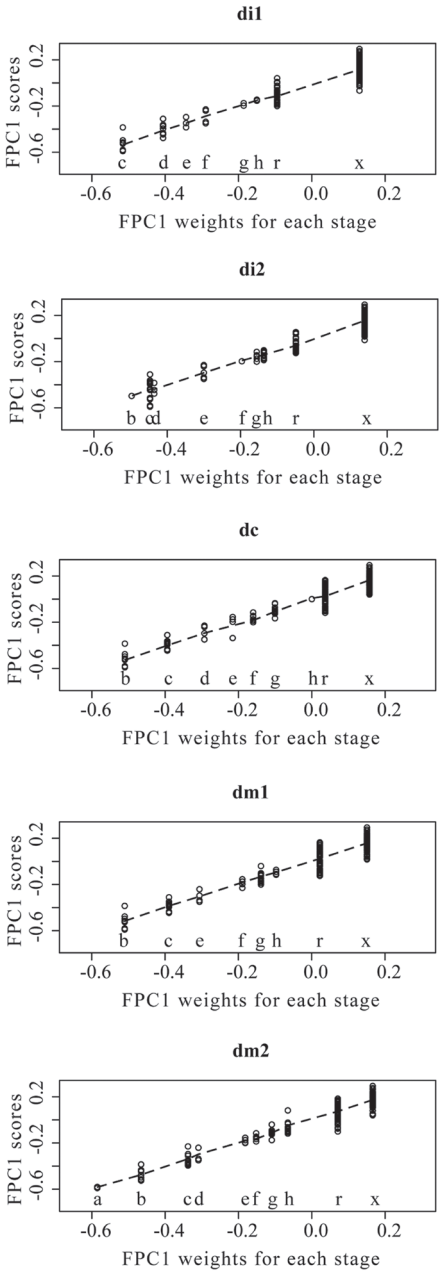

Fig. 4 - Distribution of each stage of a tooth from deciduous dentition according to their distinct FPC1 weights and FPC1 scores. Dashed lines: predicted FPC1 scores.

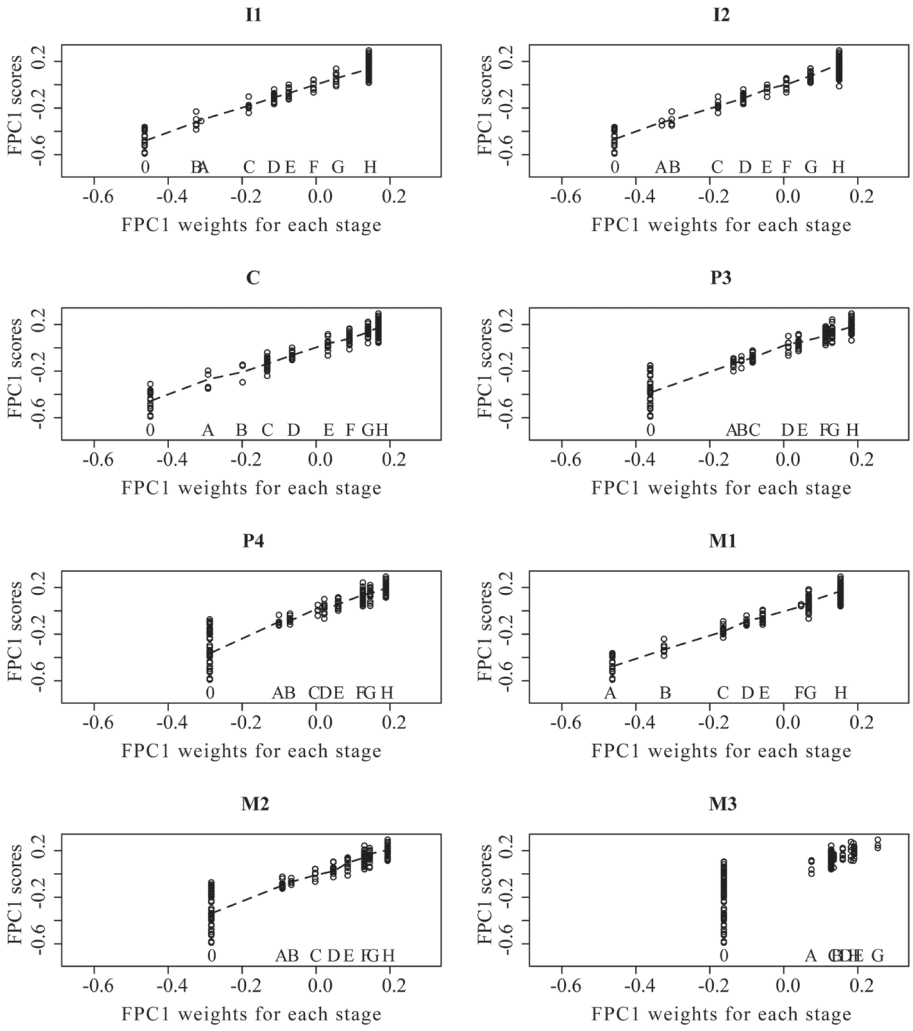

Fig. 5 - Distribution of each stage of a tooth from permanent dentition according to their distinct FPC1 weights and FPC1 scores. Dashed lines: predicted FPC1 scores.

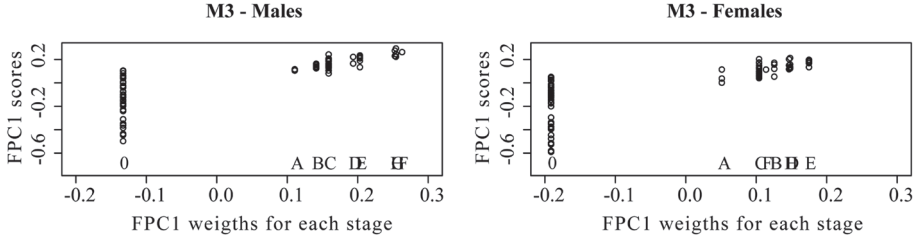

Fig. 6 - Distribution of each M3 stage to their distinct FPC1 weights and FPC1 scores in males and females.

to *C* (M1 *ABC*) (Appendix 1). The second period includes M1 stages from *D* to *H* (M1 *DEFGH*). Figure 7 plots FPC1 composite weights against the actual FPC1 scores for the pooled sample (Figs. 7a,b), for females (Figs. 7c,d), and for males (Figs. 7e,f). Dental stages appear to be well segregated along the mineralization process. The relation of mandibular form change to dental maturation was nearly perfectly linear except at the extreme of DS1 and in the second "half" of DS4. Table 3 reports that dental mineralization and mandibular form change were strongly associated within the first developmental period ($r_{pooled\ sample}$=0.976, $r_{females}$=0.981, r_{males}=0.983). Beyond this developmental period, the error variance increased substantially (Tab. 4), indicating that the association attenuated (more quickly in females, as the female error variance was twice the male error variance). Figure 7d also shows that female specimens overlapped to a greater extent from the second "half" of DS4, DS5 and DS6 than male specimens of the same dental stages (Fig. 7f). In contrast with females (Fisher test, p-value=0.024), the 95% confidence interval of the male correlation coefficient overlapped from stage M1 *ABC* to M1 *DEFGH* (Fisher test, p-value=0.186) (Tab. 4). The regression slopes are 1.002 and 0.973 for the two "halves" of the developmental process in the male subsample, and 1.030, 1.013 for the female subsample. In male and female subsamples, the slope does not change, only the error increases.

Tab. 3 - List of landmarks and curve semilandmarks shown in Figure 1.

Landmarks and curve semilandmarks	Fig. 1
Landmarks	
Infradentale	1
Linguale	2
Right mental foramen	3
Right mandibular foramen	4
Tip of the right coronoid	5
Top of the right condyle	6
Medial extremity of the right condyle	7
Lateral extremity of the right condyle	8
Curve semilandmarks	
Midsymphysis	*Sy*
Right outer alveolar	*OA*
Right inner alveolar	*IA*
Right anterior ramus	*AR*
Right coronoid	*Co*
Right inferior border	*IB*

Discussion

The present study sets out to quantify the association between teeth and mandibular form changes in living French humans across the postnatal stages. We explored size-related shape variation of these 144 living human mandibles using a dense 3D surface representation based on CT scans, we rated the dental development of these specimens, and we quantified the association between these two developmental units as it somewhat fluctuates over developmental time. The combination of geometric morphometric methods and the ACM method is a novel approach to this topic. Our principal finding is the tight association between mandibular growth and tooth development for M1 from stages *A* through *C*, during the first two years of life. Afterwards, the association weakens as indicated by the increase of the error variance (Tab. 4). To our knowledge, no other quantitative studies have investigated the association of these two developmental units.

Regarding M3, the results observed in females (Fig. 6) might correspond to the variability of its initial mineralization, as Table 5 shows a larger age range of stage *A* for females. Nevertheless, the age ranges of the four subsequent stages had comparable variances for both sexes. In males, M3 develops while mandibular form continues to change – males show extended facial growth – while in females the M3 develops inside a mandible that has already terminated its growth. Hellman (1935a,b) already noticed this in his sample of Americans.

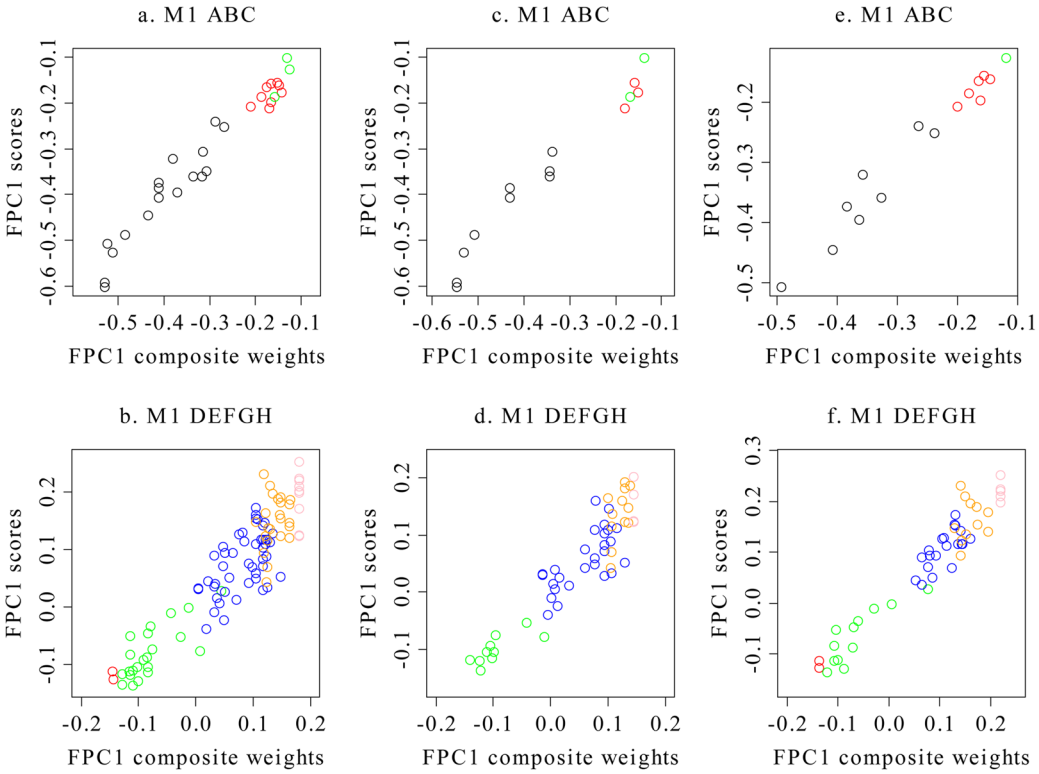

Fig. 7 - Dental development (FPC1 composite weights)** versus **mandibular form changes (FPC1 scores) for both sexes (a-b), females (c-d) and males (e-f). Two developmental periods: M1 ABC and M1 DEFGH (see Table 4 for approximate age range). Black: DS1; red: DS2; green: DS3; blue: DS4; orange: DS5; pink: DS6.

Methodological considerations

The import of our analyses arises from the creation of a metric proxy for dental development by ACM. Figure 7 shows that the relation of FPC1 to its predictor, the FPC1 composite weight, was not only monotone but also (i) nearly perfectly linear except at the extreme of DS1 and at the second half of DS4, (ii) fairly homogeneous, and furthermore (iii) nearly perfectly separated, colour cluster by colour cluster. The intermingling of FPC1 scores for the second half of DS4 with those of DS5 and DS6 suggest the limits of this approach. It would not apply to the epoch of craniofacial growth that extends past the latter events of dental development, especially in females (Fig. 7d) compared to males with their extended mandibular growth (Fig. 7f). The clear separation of DS1 from the other stages is produced by the correspondingly clear horizontal separations in the panels for the deciduous teeth (Fig. 4) and the first permanent teeth that initiate mineralization, M1, I1, I2 and C (Fig. 5). This is evidence for a stronger statistical signal than the ACM method produces: a separation where previously there were only mean differences (the FPC1 weights computed at step 2 of our analysis). The FPC1 composite weight reduces this noise while preserving the signal. This is one reason why one could prefer a

Tab. 4 Correlation coefficients between mandibular form changes (FPC1 scores) and dental development (FPC1 composite weights) computed for two developmental periods: period 1: M1 stages from A to C (M1 ABC); period 2: M1 stages from D to H (M1 DEFGH). Results are presented for the pooled sex sample, females and males. Age ranges (minimum age – maximum age) are provided for each group and developmental period. n: number of specimens included for each analysis; r: Pearson product-moment correlation coefficient; 95% CI: 95 per cent confidence interval of r.

	M1 ABC	M1 DEFGH
Pooled sex sample	**n = 29**	**n = 104**
Age range	0.0 - 2.4	2.3 - 17.0
r	0.976	0.917
95% CI	0.950 - 0.989	0.874 - 0. 937
Error variance (1-r²)	0.047	0.159
Females	**n = 14**	**n=53**
Age range	0.0 - 2.3	3.3 - 17.0
r	0.981	0.921
95% CI	0.942 - 0.994	0.867 - 0.954
Error variance (1-r²)	0.037	0.151
Males	**n = 15**	**n = 51**
Age range	0.1 - 2.4	2.3 - 17.0
r	0.983	0.962
95% CI	0.950 - 0.994	0.934 - 0.978
Error variance (1-r²)	0.033	0.074

summary scale score to the list of its component items. Moreover, the ACM has the merit of being robust against the problems of severe ceiling or floor effects, tooth by tooth, that destroyed any possibility of multilinear multivariate modelling of the tooth development treated on its own. In contrast to the current geometric morphometric methods, the use of the ACM method enables us to study the dentition as a whole, as its components come and go over ontogeny (missing teeth resulting from different times of tooth offsets, missing tooth parts resulting from mineralization and exfoliation processes, and replacement of the deciduous dentition by the permanent one). The method may thus be useful for other studies that include skeletal maturation indicators such as cervical vertebrae, hand-wrist ratings, or epiphysis closure, all of which are generally studied via categorical variables.

Relationship between tooth and mandible during development

Our results show that the first half of the total mandibular form variation (Fig. 3) is tightly bound to the developing dentition up through the complete emergence of the deciduous teeth (transition between DS2 and DS3; Figs. 7a,c,e and Tab. 4), a time when the masticatory system can process solid foods. This suggests a strict organization of associated developmental events between teeth and mandible. After birth, while the tooth buds develop and their roots elongate, the growing tooth emergences, moving the crown towards its final position above both bone and gingivae. Mandibular teeth and alveolar bone grow upward together in the course of attaining full occlusion. This is produced by an upward drift of each mandibular tooth, together with a corresponding increase in the height of the alveolar bone. The extent of this upward growth movement plus that of the downward growth movement by the maxillary arch equals the combined extent of the vertical growth of the ramus (Enlow, 1990).

Interestingly, the error variance begins to rise (Tab. 4) at the time that typically indicates early mastery of efficient and complex spoken language, approximately 2 years of age (Thibault, 2007), alongside the earlier mastication functions. Chewing development is connected to the change in the characteristic of the food consistencies, partly coded by the periodontal receptors (Dellow & Lund, 1971; Lund, 1991). In modern humans, the general coordinative organization of chewing is well established by 12 months of age (Green *et al.*, 1997), coincident with the emergence of the deciduous teeth (Bosma, 1967; Moyer, 1973). Green *et al.* (1997) observed that the onset of the activity among the jaw-elevating muscles appears to become more synchronous from approximately 2.5 years of age, the masseter

becoming the first muscle activated in the chewing cycle, as it remains in adults (Steiner *et al.*, 1974). Likewise, the adult-like rotary pattern of mandiblar movement (vertical plus lateral) is completely established sometime after 2.5 years of age (Wilson & Green, 2009). The rotary pattern begins to be expressed after the complete emergence of the deciduous molars, as the lateral jaw movements are modulated by afferent signals from receptors in or around the teeth (Takada *et al.*, 1994; Wilson & Green, 2009). This accords the general observation that tooth emergence precedes the change in chewing behaviour in mammals (Iinuma *et al.*, 1991). In summary: soon after the complete emergence of the deciduous molars, the adult pattern of mastication is achieved for efficient and complex processing of solid foods.

In parallel with mastication development, articulated language develops once the larynx and the hyoid bone have descended down the neck during postnatal life to reach the adult level at about 2 years of age (Negus, 1949; Carlsöö & Leijon, 1960; Roche & Barkla, 1965; Westhorpe, 1987). Before this moment, it has been argued that the hyo-laryngeal descent would occur simultaneously with the enlargement of the mandibular bone and the eruption of the deciduous dentition to avoid any risk of airway obstruction due to large tongue dimensions relative to the pharynx (Lieberman *et al.*, 2001). Consequently, the related mandibular components may accommodate the functional loading increase related to mastication and speech to a greater extent after about 2 years of age. This may explain why the error variance of the statistical relationship between developing teeth and the whole mandibular form change increases after the full emergence of the deciduous dentition (Tab. 4).

Also, our finding might be consistent with Boughner & Hallgrímsson's (2008) expectations about a general developmental deterioration in the fidelity of those multiple developmental "clocks". We do not have any evidence-based way to arrive at the onset of those discrepancies from cross-sectional data sets like this one. Does the gradual loss of synchronicity between the "cerebral clock" and both the "dental clock" and the "mandibular clock" correlate with the onset of an adult-like patterns of oral functions? One might expect that during the first years of life, a tight coordination between those developmental clocks might be an important condition for the achievement of adult-like patterns of function. Later in life, gradual loss of synchronization between developmental clocks would enable more plasticity in dental development and mandibular form variation in order to respond, independently or not, to the variable environmental constraints linked to diverse jaw activities during growth.

Tab. 5 - Minimum and maximum age intervals of the first five M3 tooth stages according to sex.

	F	M
A	7.5 - 10.7	8.8 - 9.2
B	7.8 - 11.3	8.3 - 11.2
C	9.9 - 13.3	10.4 - 14.5
D	11.2 - 16.2	11.0 - 14.5
E	12.9 - 17.4	12.9 - 16.3

Beyond 6 years of age, mandibular form change slows down in females (Fig. 3, bottom row). This may account for the more rapid decline of association between teeth and mandible in females (Tab. 4, Figs. 7d,f). Figure 3 also shows how male and female ontogenetic trajectories diverge beyond 6 years of age. Males are characterized by more allometric shape changes in late ontogeny as their trajectory is more aligned with FPC1. We cannot exclude the possibility that the decline of the association between teeth development and mandibular form variation in females represents a rotation of its principal component, away from the allometric direction, into the subspace of FPC2 and FPC3 (Fig. 3). Such an association may be connected with the emergence of the M3. As the female mandible has ceased to increase in size while M3 develops (Fig. 6), other developmental mechanisms may be required in order to provide room for M3 emergence. This possibility would be well worth exploring in future studies.

Finally, recent investigations on mandibular shape change and dental development in *Pan*

(Boughner & Dean, 2008) suggest that dental development does not "drive" mandibular growth in *Pan paniscus*, in contrast to *Pan troglodytes*, during late ontogeny – teeth continue to develop while the mandible has achieved its adult shape. Do the dentognathic systems differ between species because the relationship between dental development and mandibular growth weakens at different times? Further investigation on the tooth-jaw relationships in non-human primates and modern humans may yield insights to better understand the evolution of the human face.

Conclusions

This study presents a novel approach to studying the covariation between mandibular form changes and dental mineralization. Our results show a strikingly tight association between mandibular form and dental maturation up through the full emergence of the deciduous dentition, but this association lessens early during postnatal development, about 2 years of age, which is the time of the functional loading increase perhaps resulting from the concomitant learning of efficient and complex spoken language and mastication functions. Such inferences, of course, require confirmation by experiments.

Acknowledgements

This research was carried out with the support of the European project FP6 Marie Curie Actions MRTN-CT-2005-019564 (EVAN; http://www.evan.at). We thank the UMR CNRS 5199 PACEA LAPP (B. Maureille, P. Murail and M. Bessou) that provided the archaeological material from Usseau (Deux-Sèvres, France). We thank the Centre Hospitalier Universitaire Pellegrin, Bordeaux (V. Dousset, C. Douws, and C. Thiébaut), the Centre Hospitalier Universitaire Necker, Paris (F. Brunelle, N. Boddaert, and J-M. Debaets) and the Clinique Pasteur, Toulouse (J. Treil) for access to their CT datasets. We thank the Centre de Microtomographie at the Univ. of Poitiers (R. Macchiarelli, P. Sardini) and the society Etudes Recherches Matériaux (A. Mazurier) for their collaboration. We thank S. Benazzi, M. Frelat, H. Liversidge, P. Mitteroecker and S. Senck for discussion, and two anonymous reviewers for their helpful comments on an earlier draft of this manuscript. We thank A. G. Drake for discussions on earlier draft of this manuscript and for the final revision of the English language.

References

Aiello L. & Dean C. 1990. *An introduction to human evolutionary anatomy*. Academic Press, New York.

Atchley W.R. & Hall B.K. 1991. A model for development and evolution of complex morphological structures. *Biol. Rev. Camb. Philos. Soc.*, 66: 101-157.

Başaran G., Özer T. & Hamamci N. 2007. Cervical vertebral and dental maturity in Turkish subjects. *Am. J. Orthod. Dentofacial Orthop.*, 131: 447.e13–447.e20.

Bayle P., Braga J., Mazurier A. & Macchiarelli R. 2009a. Brief Communication: high-resolution assessment of the dental developmental pattern and characterization of tooth tissue proportions in the late Upper Paleolithic child from la Madeleine, France. *Am. J. Phys. Anthropol.*, 138: 493-498

Bayle P., Braga J., Mazurier A. & Macchiarelli R. 2009b. Dental developmental pattern of the Neanderthal child from Roc de Marsal: a high-resolution 3D analysis. *J. Hum. Evol.*, 56: 66-75.

Bastir M. & Rosas A. 2004. Facial heights: evolutionary relevance of postnatal ontogeny for facial orientation and skull morphology in humans and chimpanzees. *J. Hum. Evol.*, 47: 359-381.

Bastir M. & Rosas A. 2006. Correlated variation between the lateral basicranium and the face: a geometric morphometric study in different human groups. *Arch. Oral Biol.*, 51: 814-824.

Bastir M. 2008. A systems-model for the morphological analysis of integration and modularity in human craniofacial evolution. *J. Anthropol. Sci.*, 86: .37-58.

Bookstein F.L. 1991. *Morphometric tools for landmark data: geometry and biology*. Cambridge University Press, Cambridge, New York.

Bookstein F.L. 1997. Landmark methods for forms without landmarks: morphometrics of group differences in outline shape. *Med. Image Anal.*, 1: 225-243.

Bookstein F.L., Sampson P.D., Streissguth A.P. & Barr H.M. 1996. Exploiting redundant measurement of dose and developmental outcome: new methods from behavioural teratology of alcohol. *Dev. Psychol.*, 32:404-415.

Bookstein F.L. & Green W.D.K. 2002. *Users Manual, EWSH3.19*. ftp://brainmap.med.umich.edu/pub/ewsh.3.19.manual.

Bookstein F.L., Gunz P., Mitteroecker P., Prossinger H., Schaefer K. & Seidler H. 2003. Cranial integration in Homo: singular warps analysis of the midsagittal plane in ontogeny and evolution. *J. Hum. Evol.*, 44: 167-187.

Boughner J.C. & Hallgrímsson B. 2008. Biological spacetime and the temporal integration of functional modules: a case study of dento-gnathic developmental timing. *Dev. Dyn.*, 237: 1-17.

Boughner J.C. & Dean M.C. 2008. Mandibular shape, ontogeny and dental development in Bonobos (*Pan paniscus*) and Chimpanzees (*Pan troglodytes*). *Evol. Biol.*, 35: 296-308.

Bosma J.F. 1967. Human infant oral functions. In J.F. Bosma (ed): *Symposium on oral sensation and perception*, pp. 107-108. C.C. Thomas Publishers, Springfield.

Braga J. & Heuzé Y. 2007. Quantifying variation in human dental developmental sequences. An Evo-Devo perspective. In S.E. Bailey, J-J. Hublin (eds): *Dental perspectives on human evolution: state of the art research in dental anthropology*, pp. 247-261. Springer, Berlin.

Bulygina E., Mitteroecker P. & Aiello L. 2006. Ontogeny of facial dimorphism and patterns of individual development within one human population. *Am. J. Phys. Anthropol.*, 131: 432-443.

Carlsöö S. & Leijon G. 1960. A radiographic study of the position of the hyo-laryngeal complex in relation to the skull and the cervical column in man. *Trans. R. Sch. Dent. Umea. (Stockh)*, 5: 13-35.

Cobb S.N. & O'Higgins P. 2007. The ontogeny of sexual dimorphism in the facial skeleton of African apes. *J. Hum. Evol.*, 53: 176-190.

Cobb S.N. & Baverstock H. Tooth root and craniomandibular morphological integration in the common chimpanzee (*Pan troglodytes*): alternative developmental models for the determinants of root length. *Front. Oral Biol.*, 13: 121-127.

Coquerelle M., Bayle P., Heuzé Y., Mazurier A. & Braga J. 2007. Assessment of the dental developmental status of an individual. Adaptability of radiographic scoring systems of mineralisation stages to (micro)CT? *Bull. Mém. Soc. Anthropol. Paris*, 19: 4.

Dean M.C. & Wood B.A. 1981. Developing pongid dentition and its use for aging individual crania in comparative cross-sectional growth studies. *Folia Primatol.*, 36: 111-127.

Dean M.C. 2006. Tooth microstructure tracks the pace of human life-history evolution. *Proc. R. Soc. Lond. B. Sci.*, 273: 2799-2808.

Dellow P.G. & Lund J.P. 1971. Evidence for central timing rhythmical mastication. *J. Physiol.*, 215: 1-13.

Demirjian A., Goldstein H. & Tanner J.M. 1973. A new system of dental age assessment. *Hum. Biol.*, 45: 211-227.

Dryden I.L. & Mardia K.V. 1998. *Statistical shape analysis*. John Wiley and Sons, New York.

Enlow D.H. 1990. *Facial growth*. W.B. Saunders Company, Philadelphia.

Fant G. 1960. *Acoustic theory of speech production*. Mouton, The Hague.

Green J.R., Moore C.A., Ruark J.L., Rodda P.R., Morvee W.T. & VanWitzenburg M.J. 1997. Development of chewing in children from 12 to 48 months: longitudinal study of EMG patterns. *J. Neurophysiol.*, 77: 2704-2716.

Gunz P., Mitteroecker P. & Bookstein F.L. 2005. Semilandmarks in three dimensions. In D.E. Slice (ed): *Modern Morphometrics in Physical Anthropology*, pp. 73-98. Kluwer Academic/ Plenum Publishers, New York.

Gunz P. & Harvati K. 2007. The Neanderthal "chignon": variation, integration and homology. *J. Hum. Evol.*, 52:262-274.

Hellman M. 1935a. The face in its developmental career. *Dent. Cosm.*, 77: 685-699.

Hellman M. 1935b. The face in its developmental career. *Dent. Cosm.*, 77: 777-787.

Heuzé Y. 2004. *Chronologie et étiologie de la maturation macrostructurale des dents définitives*. Thèse de Doctorat. Université Bordeaux 1, Talence.

Iinuma M., Yoshida S. & Funakoshi M. 1991. Development of masticatory muscles and oral behavior from suckling to chewing in dogs. *Comp. Biochem. Physiol.*, 100:789-794.

Krantz D.H., Luce R.D., Suppes P. & Tversky A. 1971. *Foundations of measurement.* Academic Press, New York.

Kupczik K., Dobson C.A., Crompton R.H., Phillips R., Oxnard C.E, Fagan M.J. & O'Higgins P. 2009. Masticatory loading and bone adaptation in the supraorbital torus of developing macaques. *Am. J. Phys. Anthropol.*, 139: 193-203.

Kurihara S., Enlow D.H. & Rangel R.D. 1980. Remodeling reversals in anterior parts of the human mandible and maxilla. *Angle Orthod.*, 50: 98-106.

Lieberman D.E. & McCarthy R.C. 1999. The ontogeny of cranial base angulation in humans and chimpanzees and its implications for reconstructing pharyngeal dimensions. *J. Hum. Evol.*, 36: 487-517.

Lieberman D.E., McCarthy R.C., Hiiemae K.M. & Palmer J.B. 2001. Ontogeny of postnatal hyoid and larynx descent in humans. *Arch. Oral Biol.*, 46: 117-128.

Liversidge H.M. & Molleson T. 2004. Variation in crown and root formation and eruption of human deciduous teeth. *Am. J. Phys. Anthropol.*, 123: 172-180.

Luce R.D. & Tukey J.W. 1964. Simultaneous conjoint measurement: a new type of fundamental measurement. *J. Math. Psychology*, 1: 1-27.

Lumsden A.G.S. 1988. Spatial organization of the epithelium and the role of neural crest cells in the initiation of the mammalian tooth germ. *Development*, 103: 155-169.

Lund J.P. 1991. Mastication and its control by the brain stem. *Crit. Rev. Oral Biol. Med.*, 2: 33-64.

McClean M.D. & Tasko S.M. 2003. Association of orofacial muscle activity and movement during changes in speech rate and intensity. *J. Speech Lang. Hear Res.*, 46: 1387-1400.

McNamara J.A. & Graber L.W. 1975. Mandibular growth in the Rhesus monkey (*Macaca mulatta*). *Am. J. Phys. Anthropol.*, 42: 15-24.

Mitteroecker P., Gunz P., Bernhard M., Schaefer K. & Bookstein F.L. 2004. Comparison of cranial ontogenetic trajectories among great apes and humans. *J. Hum. Evol.*, 46: 679-698.

Mitteroecker P. & Bookstein F. 2007. The conceptual and statistical relationship between modularity and morphological integration. *Syst. Biol.*, 56: 818-836.

Mitteroecker P. & Bookstein F. The evolutionary role of modularity and integration in the hominoid cranium. *Evolution*, 62: 943-958.

Moore C.A., Smith A. & Ringel R.L. 1988. Task-specific organization of activity in human jaw muscles. *J. Speech Lang. Hear Res.*, 31: 670-680.

Moorrees C.F., Fanning E.A & Hunt E.E. 1963. Age variation of formation stages for ten permanent teeth. *J. Dent. Res.*, 42: 1490-1502.

Moss M.L. & Young R.W. 1960. A functional approach to craniology. *Am. J. Phys. Anthropol.*, 18: 281-292.

Moss M.L. 1962. The functional matrix. In B.S Krauss & R.A. Riedel (eds): *Vistas in orthodonctics,* pp. 85-98. Philadelphia.

Moyers R.E. 1973. *Handbook of orthodontics. 3rd Edition*. Year Book Medical Publishers, Chicago.

Negus V.E. 1949. *The comparative anatomy and physiology of the larynx*. Hafner, New York.

Nissen H.W. & Riesen A.H. 1945. The deciduous dentition of chimpanzee. *Growth*, 9: 265-274.

Nissen H.W. & Riesen A.H. 1964. The eruption of the permanent dentition in the chimpanzee. *Am. J. Phys. Anthropol.*, 22: 285-294.

Roche A.F. & Barkla D.H. 1965. The level of the larynx during childhood. *Ann. Otol. Rhinol. Laryngol.*, 74: 645-654.

Pinder G.L. & Faherty A.S. 1999. Issues in pediatric feeding and swallowing. In A.J Caruso & A. Strand (eds): *Clinical management of motor*

speech disorders in children, pp. 281-318. Thieme Medical Publishers, New York.

Robinow M., Richards T.W. & Anderson M. 1942. The eruption of deciduous teeth. *Growth*, 6:127-133.

Rohlf F.J. & Slice D.E. 1990. Extensions of the procrustes method for the optimal superimposition of landmarks. *Syst. Zool.*, 39: 40-59.

Rohlf F.J. & Corti. M. 2000. The use of two-block partial least-squares to study covariation in shape. *Syst. Biol.*, 49: 740-753.

Shea B.T. 1989. Heterochrony in human evolution: the case for neoteny reconsidered. *Yearb. Phys. Anthropol.*, 32: 69-101.

Schultz A.H. 1935. Eruption and decay of the permanent teeth in primates. *Am. J. Phys. Anthropol.*, 19: 489-581.

Schwartz G.T. & Dean C. 2000. Interpreting the hominid dentition: ontogenetic and phylogenetic aspects. In P. O'Higgins & M.J. Cohn (eds): *Development, growth and evolution. Implications for the study of the hominid skeleton*. pp. 207-233. Academic press, London.

Spoor F., Zonneveld F. & Macho G.A. 1993. Linear measurements of cortical bone and dental enamel by computed tomography: applications and problems. *Am. J. Phys. Anthropol.*, 91: 469-484.

Steiner J.E., Michman J. & Litman A. 1974. Time sequence of the activity of the temporal and masseter muscles in healthy young human adults during habitual chewing of different test foods. *Arch. Oral Biol.*, 19: 29-34.

Takada K., Miyawaki S. & Tatsuta M. The effects of food consistency on jaw movement and posterior temporalis and inferior orbicularis oris muscle activities during chewing in children. *Arch. Oral Biol.*, 39: 793-805.

Thilbault C. 2007. *Orthophonie et oralité: la sphère oro-faciale de l'enfant*. Elsevier Masson, Paris.

Uysal T., Sari Z., Ramoglu S.I. & Basciftci F.A. 2004. Relationships between dental and skeletal maturity in Turkish subjects. *Angle Orthod.*, 74: 657-664.

Westhorpe R.N. 1987. The position of the larynx in children and its relationship to the ease of intubation. *Anaesthes. Int. Care*, 15: 384-388.

Wildgruber D., Ackermann H. & Grodd W. 2001. Differential contributions of motor cortex, basal ganglia, and cerebellum to speech motor control: Effects of syllable repetition rate evaluated by fMRI. *Neuroimage*, 13: 101-109.

Wilson E.M, Green J.R., Yunusova Y.Y. & Moore C.A. 2008. Task specificity in early oral motor development. *Semin. Speech Lang.*, 29: 257-266.

Wilson E.M. & Green J.R. 2009. The development of jaw motion for mastication. *Early Hum. Dev.*, 85: 303-311.

Associate Editor, Markus Bastir

Appendix 1 - Exclusive dental sequences sorted according to the increment of FPC1 composite weights for the pooled-sex group. n: number of times the sequence is represented in the sample. M3 is not included in the table.

Sequences	FPC1 composite weights	Age	DS	di1	di2	dc	dm1	dm2	I1	I2	C	P1	P2	M1	M2	n
1	-0.53	0.0	1	c	c	b	b	a	0	0	0	0	0	A	0	2
2	-0.52	0.3	1	c	b	b	b	b	0	0	0	0	0	A	0	1
3	-0.51	0.1	1	c	c	b	b	b	0	0	0	0	0	A	0	1
4	-0.48	0.2	1	d	d	b	b	b	0	0	0	0	0	A	0	1
5	-0.44	0.2	1	d	c	c	c	b	0	0	0	0	0	A	0	1
6	-0.41	0.3	1	d	c	c	c	c	0	0	0	0	0	A	0	3
7	-0.38	0.4	1	d	c	c	c	c	A	A	0	0	0	B	0	1
8	-0.37	1.2	1	e	d	c	c	c	B	0	0	0	0	B	0	1
9	-0.34	0.6	1	e	e	d	c	c	B	A	A	0	0	B	0	1
10	-0.32	1.1	1	f	e	d	e	d	B	B	A	0	0	B	0	1
11	-0.32	0.9	1	e	e	d	e	c	B	B	B	0	0	B	0	1
12	-0.31	0.7	1	f	e	e	e	d	B	B	A	0	0	B	0	1
13	-0.29	1.1	1	f	e	d	f	c	B	B	A	0	0	C	0	1
14	-0.27	0.8	1	f	e	d	e	d	C	C	C	0	0	B	0	1
15	-0.21	1.3	2	g	f	e	f	e	C	C	A	0	0	C	0	1
16	-0.19	1.5	2	g	g	e	f	e	C	C	C	0	0	C	0	1
17	-0.18	1.4	2	h	g	e	f	e	D	D	B	0	0	C	0	1
18	-0.17	1.4	2	r	g	f	g	e	C	C	C	A	0	C	0	1
19	-0.17	1.7	2	r	h	f	g	f	C	C	C	0	0	C	0	1
20	-0.17	2.1	2	r	g	f	g	f	D	C	B	A	0	C	0	1
21	-0.16	2.3	3	r	h	f	g	g	C	C	C	B	0	C	0	1
22	-0.15	2.1	2	h	g	f	g	f	D	D	C	A	0	C	0	1
23	-0.15	2.3	2	r	h	f	g	f	D	D	C	0	0	C	0	1
24	-0.15	2.3	2	r	h	g	g	g	C	C	C	A	0	D	0	1
25	-0.15	2.7	2	r	g	f	g	f	D	D	C	A	0	D	0	1
26	-0.14	2.1	2	r	h	g	g	f	D	D	C	A	0	C	0	1
27	-0.13	2.3	3	r	r	g	h	g	D	D	C	A	0	C	0	1
28	-0.13	3.0	3	r	h	g	g	g	D	D	C	A	A	D	0	1
29	-0.13	3.3	3	r	h	g	g	g	D	D	C	B	0	D	0	1
30	-0.13	2.4	3	r	h	g	h	h	D	D	C	B	0	C	0	1
31	-0.12	2.5	3	r	h	g	r	g	D	D	D	B	A	D	0	1
32	-0.12	3.3	3	r	r	g	h	h	D	D	C	B	0	D	0	1
33	-0.12	2.7	3	r	r	g	g	g	D	D	C	C	B	D	A	1
34	-0.12	3.5	3	r	r	g	h	g	D	D	C	C	0	D	A	1
35	-0.11	3.8	3	r	r	g	r	g	E	D	C	C	A	D	A	1
36	-0.11	3.9	3	r	r	r	r	r	E	D	C	C	A	D	A	1
37	-0.10	3.8	3	r	r	r	r	h	D	D	D	C	A	D	A	1
38	-0.10	3.6	3	r	r	r	r	h	E	D	C	C	A	E	A	1

Appendix 1 (continued)

Sequences	FPC1 composite weights	Age	DS	di1	di2	dc	dm1	dm2	I1	I2	C	P1	P2	M1	M2	n
39	-0.09	3.8	3	r	r	r	r	h	D	D	D	C	B	E	A	1
40	-0.09	4.0	3	r	r	r	r	r	E	D	D	C	B	E	B	1
41	-0.08	4.3	3	r	r	r	r	h	E	D	D	C	B	E	B	1
42	-0.08	3.9	3	r	r	g	r	h	E	E	D	C	A	E	B	1
43	-0.08	4.0	3	r	r	r	r	h	E	E	D	C	A	E	A	1
44	-0.08	3.9	3	r	r	r	r	h	E	E	D	C	B	E	A	1
45	-0.08	4.1	3	r	r	r	r	h	E	E	D	C	B	E	B	1
46	-0.04	5.1	3	r	r	h	r	r	E	E	D	D	C	E	C	1
47	-0.03	5.4	3	r	r	r	r	r	F	F	D	D	C	E	C	1
48	-0.01	5.9	3	r	r	r	r	r	F	F	E	D	C	E	C	1
49	0.00	6.7	4	x	r	r	r	r	F	F	E	D	D	F	C	2
50	0.01	6.0	3	x	r	r	r	r	F	F	E	D	D	G	C	1
51	0.02	7.1	4	x	r	r	r	r	F	F	E	E	D	G	D	1
52	0.02	7.8	4	x	r	r	r	r	H	F	E	E	D	F	D	1
53	0.03	7.4	4	x	r	r	r	r	G	F	E	E	E	G	D	2
54	0.03	7.7	4	x	x	r	r	r	G	G	E	D	D	G	D	1
55	0.03	7.6	4	x	x	r	r	r	G	G	E	E	C	G	D	1
56	0.04	7.6	4	x	x	r	x	r	G	G	E	E	D	G	D	1
57	0.04	8.7	4	x	x	r	x	r	H	G	E	E	E	G	D	1
58	0.04	5.4	3	x	x	r	r	r	H	G	F	E	D	G	D	1
59	0.05	8.8	4	x	x	r	r	r	H	G	E	E	E	G	E	1
60	0.05	8.3	4	x	x	r	r	h	G	G	F	F	E	G	E	1
61	0.05	7.6	4	x	x	r	r	r	G	H	F	E	D	G	E	1
62	0.05	8.5	4	x	x	r	r	r	H	G	F	E	E	G	D	2
63	0.06	8.1	4	x	x	r	r	r	H	G	F	E	E	G	E	1
64	0.06	9.0	4	x	x	r	r	r	H	H	F	F	E	G	D	1
65	0.07	8.6	4	x	x	r	x	r	H	G	F	F	E	G	E	1
66	0.07	8.5	4	x	x	r	r	r	G	G	F	F	F	G	E	1
67	0.08	8.3	4	x	x	r	r	r	H	G	F	F	F	G	E	1
68	0.08	8.7	4	x	x	r	r	r	H	H	F	F	F	G	E	1
69	0.09	9.0	4	x	x	r	r	r	H	H	F	F	F	H	E	2
70	0.10	10.4	4	x	x	r	x	x	H	H	F	G	F	G	F	1
71	0.10	11.6	4	x	x	x	x	r	H	H	F	F	F	H	F	5
72	0.10	10.8	4	x	x	x	x	r	H	H	G	F	F	G	F	2
73	0.11	9.6	4	x	x	r	r	r	H	H	F	G	F	H	F	1
74	0.11	11.7	4	x	x	x	x	x	H	H	G	G	G	H	E	1
75	0.12	11.0	4	x	x	x	x	r	H	H	G	F	F	H	F	7
76	0.12	13.4	5	x	x	x	x	x	H	H	H	G	F	H	F	2
77	0.12	11.3	4	x	x	r	r	r	H	H	G	F	F	H	G	1

Appendix 1 (continued)

Sequences	FPC1 composite weights	Age	DS	di1	di2	dc	dm1	dm2	I1	I2	C	P1	P2	M1	M2	n
78	0.12	11.2	4	x	x	x	x	x	H	H	G	G	F	H	F	4
79	0.12	10.9	4	x	x	x	x	r	H	H	H	G	F	H	G	2
80	0.12	11.7	4	x	x	x	x	r	H	H	G	G	F	H	G	1
81	0.12	12.2	4	x	x	x	x	x	H	H	H	G	G	H	F	3
82	0.13	10.8	5	x	x	x	x	x	H	H	G	G	G	H	F	1
83	0.13	11.0	5	x	x	x	x	x	H	H	G	G	G	H	G	1
84	0.13	12.4	4	x	x	x	x	x	H	H	H	G	G	H	G	2
85	0.13	11.7	4	x	x	x	x	x	H	H	G	H	F	H	F	2
86	0.14	12.5	5	x	x	x	x	x	H	H	H	H	G	H	F	1
87	0.15	12.1	5	x	x	x	x	x	H	H	H	G	G	H	H	1
88	0.15	13.0	4	x	x	x	x	r	H	H	H	H	G	H	G	5
89	0.16	13.4	5	x	x	x	x	x	H	H	H	H	H	H	G	4
90	0.16	14.1	5	x	x	x	x	x	H	H	H	H	G	H	H	1
91	0.18	15.2	6	x	x	x	x	x	H	H	H	H	H	H	H	21